JOURNAL OF THEORETICAL
AND APPLIED MECHANICS
40, 4, pp. 1051-1074, Warsaw 2002

COMPARISON OF MODELS FOR DYNAMIC ANALYSIS OF A MOBILE TELESCOPIC CRANE

ANDRZEJ MACZYŃSKI
MAREK SZCZOTKA

Department of Mechanical Engineering and Informatics, University of Bielsko-Biała
amaczyński@ath.bielsko.pl; mszczotka@ath.bielsko.pl

The paper compares two models of a mobile telescopic crane. The first is analytical and uses methods common in manipulator dynamics together with the modal method; the second uses the commercial ADAMS® package. Results of numerical simulations for rotation of the crane upper structure are presented and compared. Models are evaluated in terms of calculation time, possible development and use in crane design.

Key words: crane, modelling, dynamic analysis, verification

1. Introduction

Numerical dynamic analysis of machines and mechanisms can only be carried out if mathematical models are appropriate. A range of simplifying assumptions are made in a model, depending on the problem to be solved. Generally speaking, models should be as simple as possible in order to ensure numerical effectiveness. It is also important to remember that when developing a simple model the risk of error is reduced. Nevertheless, the model must sufficiently reflect the actual features of the system investigated. It always needs to be borne in mind that oversimplification or some other kind of error makes the obtained results not exact enough for a usefull analysi. Therefore, verification is essential. The best, but most expensive and labour-intensive, verification is experimental, which requires both appropriate testing and measurement apparatus, and access to the actual object of research. This is often beyond the financial means of the research institution. In addition, if the product is at the project or design stage, the actual object does not exist at all

and so experimental measurements are impossible. A substitute method is numerical verification, which involves carrying out the same dynamic analysis for two or more models obtained by different methods.

In many papers dealing with the problem of modelling of mobile cranes, their assemblies and other machines whose design includes similar solutions which depend on formulation of the problem, different approaches are considered. There are 2D (Chwastek and Michałowski, 2001; Grabski et al., 1993; Harlecki, 1998) as well as 3D (Grabski et al., 1994; Majewski and Trombski, 1993; Trombski et al., 1990) models for analysis of slewing motion. These models frequently have several up to over a dozen degrees of freedom. Different phenomena, for example flexibilities of elements, damping and backlashes are considered in description of particular systems. The 3D model presented in Chwastek and Michałowski (2000) can be used for analysis of a crane, and thus frame loads are not typical when one wheel runs over an obstacle of a specified geometry. The problems of the ground rheology are also discussed. Towarek (1996b), Towarek and Trombski (1993, 1994) consider lifting motion of the load, while papers (Towarek, 1996a; Trombski and Towarek, 1997) deal with slewing motion. Those models are often used for tasks related to steering (Kłosiński, 2002; Lubnaer et al., 1996; Parker et al., 1995a,b; Sakawa and Nakazumi, 1985; Sakawa et al., 1981; Tanizumi et al., 1995; Trombski et al., 1995, 1999).

A telescopic jib is treated in various ways, i.e. as a rigid rod (Towarek, 1996a,b; Kłosiński, 2002), one flexible beam (Lubnauer et al., 1996), a system of beams working together (Kukla et al., 1994; Maczyński and Suwaj, 1993; Posiadała et al., 1991, 2000), and different methods are used for discretisation, for exapmple FEM (Maczyński, 1998), or Rigid Finite Element method (RFEM) (Harlecki, 1998).

Similar problems of modelling are also solved for other types of cranes. Simple 2D models of off- and on-shore cranes are presented in Osiński and Wojciech (1994, 1996, 1998), while 3D models of on-shore cranes are discussed in Kościelny and Wojciech (1994), Parker et al. (1999a,b). Ho-Hoon (1998) presents a dynamic model of a three-dimensional overhead crane.

This paper will numerically verify the dynamic model of the mobile telescopic crane presented in Maczyński and Kościelny (1999). The model for comparative purposes was developed using the ADAMS® package. The ANSYS® system was used to model the jib. The rotation of the upper structure was verified. The assumed drive function was optimized in terms of minimizing final load oscillations according to the algorithm given in Maczyński and Wojciech (2000).

2. Description of the analytical model

The 3D model of a mobile telescopic crane is presented in Fig. 1. It is designed for universal dynamic analysis of cranes and takes into account:

A) different types of motion:

- slewing of an upper structure (angle φ),
- lifting and lowering of a load by means of the hoisting winch (angle α),
- change of the crane radius (angle ψ),

B) flexibility of: supports, jib, rope system, drives,

C) damping of: supports, rope system, drives.

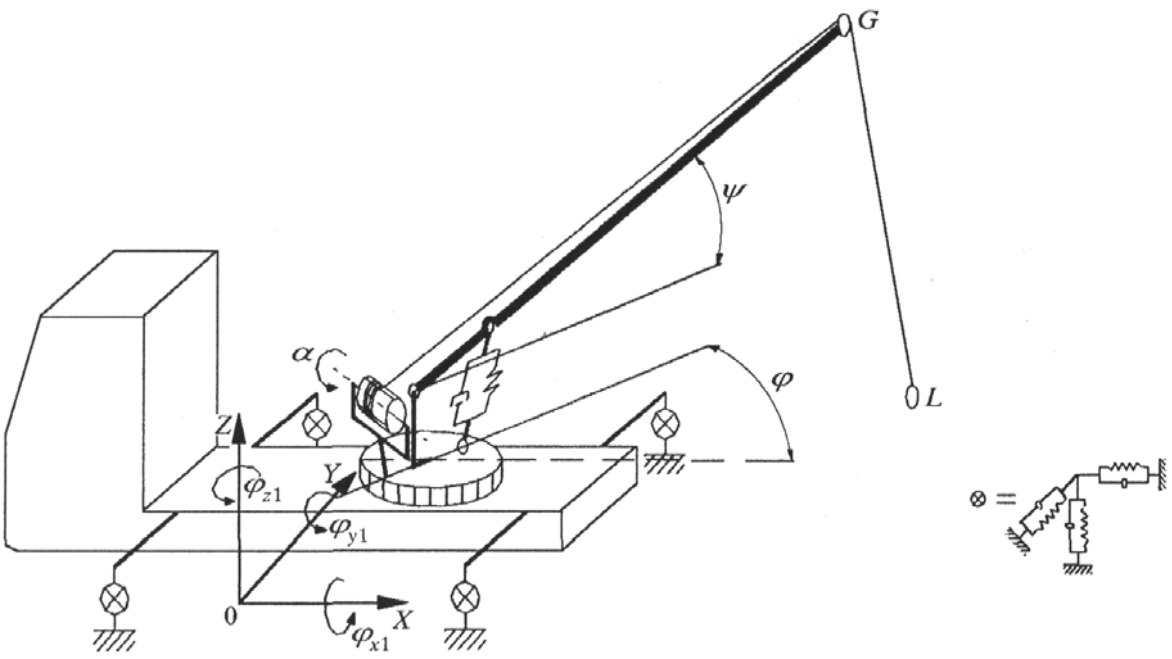

Fig. 1. Model of a mobile crane

In preparing the model, the possibility of telescopic extension of the jib has been neglected because it is a motion which is rarely considered by producers as a working motion (i.e. motion performed under the effective loading). The following assumptions have been made:

- the chassis of the crane is modelled as a solid body with 6 degrees of freedom,

- the slewing (rotation) angles $\varphi_{x1}, \varphi_{y1}, \varphi_{z1}$ of chassis are small,
- flexibility and damping in the supports are taken into consideration,
- the upper slewing structure was considered as a solid body,
- the telescopic jib is modelled as a flexible element with respect to bending,
- for the load displacements only oscillations of the jib in lifting and perpendicular planes are essential,
- oscillations of the jib in both planes are independent,
- flexibility and damping of the servo-motor changing the radius is taken into consideration,
- the jib slope angle ψ changes with length of the servo-motor,
- flexibility and damping of the hoisting rope are taken into consideration,
- the rope is considered as massless and limp,
- the load can be in contact the ground, which enables the phases of taking up and putting down (lifting/jacking up/placing) to be analysed,
- the input of the slewing motion of the upper structure and the drum of the hoisting winch is considered as the kinematic input via a spring damper.

The modal method, based upon the finite element method (FEM) (Wojciech, 1993), was used to model the jib. The method considerably reduces the number of degrees of freedom of the model, but its basic dynamic properties are still preserved (first m frequencies and forms of free vibrations). Coordinate systems in the model are chosen according to the Denavit-Hartenberg notation. The equations of motion of the crane are derived from the Lagrange equations of the second order, as follows

$$\varepsilon_k + \frac{\partial V}{\partial q_k} + \frac{\partial D}{\partial q_k} = Q_k \qquad k = 1, ..., n \tag{2.1}$$

where

$$\varepsilon_k = \frac{d}{dt}\frac{\partial E}{\partial \dot{q}_k} - \frac{\partial E}{\partial q_k}$$

and

E – kinetic energy of the system
V – potential energy of the system
D – function of energy dissipation
Q_k – non-potential generalized forces
$\boldsymbol{q}$ – vector of generalized coordinates, $\boldsymbol{q} = [q_1, ..., q_n]^\top$.

In the following sections subsystems of the model are briefly presented.

2.1. Chassis model

The coordinate system $0XYZ$ is a base system (inertial) and the coordinate system $0_1X_1Y_1Z_1$ is strictly assigned to the chassis (Fig. 2). The vector of generalized coordinates for the chassis is expressed in the following form

$$\boldsymbol{q}_c = [q_1, ..., q_6]^\top = [x_{01}, y_{01}, z_{01}, \varphi_{x1}, \varphi_{y1}, \varphi_{z1}]^\top$$

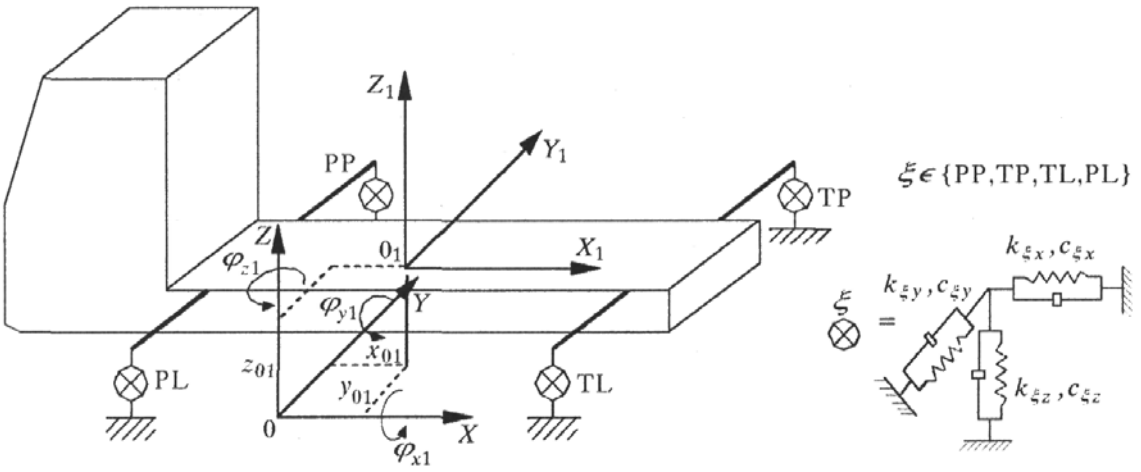

Fig. 2. Model of chassis

The vector of position of a particular point, determined in the movable coordinate system $0_1X_1Y_1Z_1$, can be presented in the inertial coordinate system $0XYZ$ by the following formula

$$\boldsymbol{r} = {}^0_1\mathbf{B} \cdot \boldsymbol{r}_1 \tag{2.2}$$

where

- $\boldsymbol{r}_1$ – position vector determined in the coordinate system $0_1X_1Y_1Z_1$, $\boldsymbol{r}_1 = [x_1, y_1, z_1, 1]^\top$
- $\boldsymbol{r}$ – position vector determined in the coordinate system $0XYZ$, $\boldsymbol{r} = [x, y, z, 1]^\top$
- ${}^0_1\mathbf{B}$ – matrix operator 4×4 called homogeneous transformation.

The kinetic energy of the chassis can be calculated as

$$E_1 = \frac{1}{2} \int\limits_{m_1} \dot{\boldsymbol{r}}^\top \cdot \dot{\boldsymbol{r}} \, dm_1 = \frac{1}{2} \int\limits_{m_1} \operatorname{tr}(\dot{\boldsymbol{r}} \cdot \dot{\boldsymbol{r}}^\top) \, dm_1 \tag{2.3}$$

where m_1 – mass of the chassis.

The potential energy of the chassis is a sum of the potential energy of the forces of gravity V_{1p} and the potential energy of the flexibility of the support V_{1s}

$$V_1 = V_{1p} + V_{1s} \tag{2.4}$$

where

$$V_{1p} = m_1 g z_{01} \qquad V_{1s} = \frac{1}{2}\sum_{i=1}^{12} c_i \Delta_i^2$$

and

c_i – stiffness coefficients of the ith support (Fig. 2)
Δ_i – deflection of the ith support.

2.2. Models of the upper structure and jib

The coordinate system $0_2X_2Y_2Z_2$ assigned to the upper slewing structure, coordinate system $0_3X_3Y_3Z_3$ assigned to the rigid part of the jib, and coordinate system $0_4X_4Y_4Z_4$ assigned to the flexible part of the jib are presented in Fig. 3 (for the sake of clarity the descriptions of origins of the coordinate systems 0_2, 0_3 and 0_4 are omitted). Angle denotations are as follows: φ – slewing angle of the upper structure, ψ – slope angle of the jib.

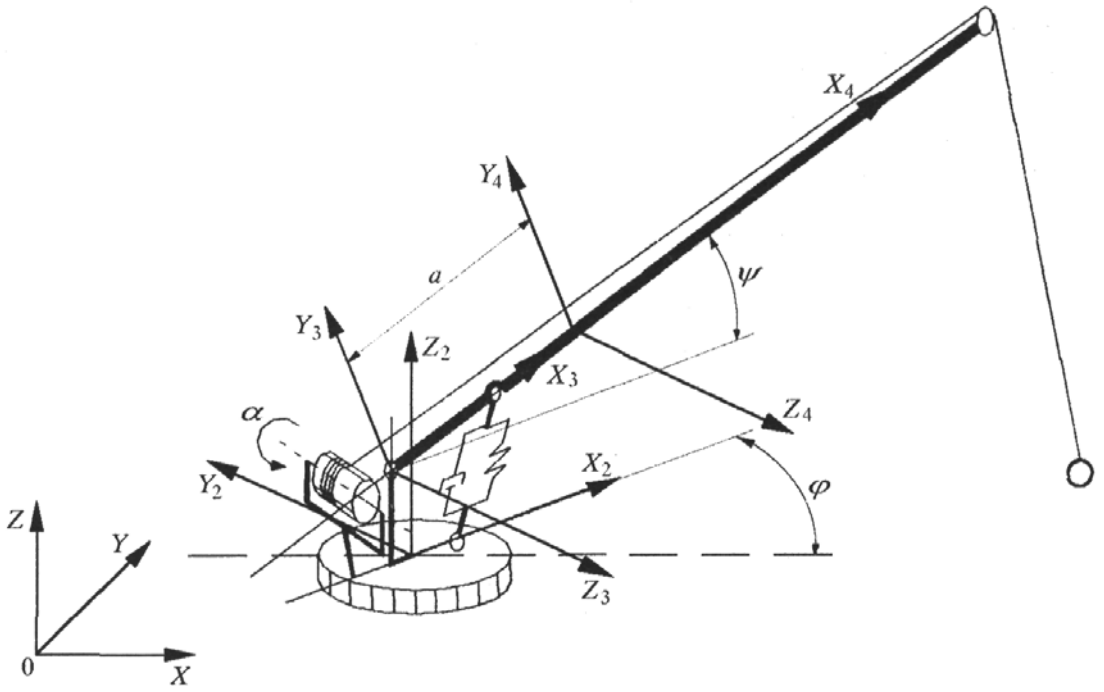

Fig. 3. Model of upper structure

The telescopic jib is a standard system with continuous mass distribution. In the paper, the modal method based upon the finite element method is used for its discretisation. The jib modelled as a supporting beam with a variable cross-section is assumed. The deflection of a particular point of the jib can be written in the following form

$$u_{y4} = \sum_{i=1}^{e_y} f_{yi}(t) N_{yi}(x_4)$$
$$u_{z4} = \sum_{i=1}^{e_z} f_{zi}(t) N_{zi}(x_4) \tag{2.5}$$

where

f_{yi}, f_{zi} – unknown functions of time

N_{yi}, N_{zi} – known functions of the coordinate x_4, chosen such that boundary and continuity conditions are fulfilled

e_y, e_z – numbers of degrees of freedom in planes $0_4X_4Y_4$ and $0_4X_4Z_4$.

It is assumed in further considerations that the frequencies and forms of free vibrations of the jib are known. The problem described has been solved twice by means of the finite element method, i.e. using the ANSYS system and using our own computer programmes. Taking into account the assumption that in the dynamic analysis it is enough to keep only m_y and m_z forms of the free vibrations (in the planes $0_4X_4Y_4$ and $0_4X_4Z_4$, respectively), after simple transformations the slope of the jib can be presented by the following formula

$$u_{y4} = \sum_{i=1}^{m_y} \eta_{yi}(t) S_{yi}(x_4)$$
$$u_{z4} = \sum_{i=1}^{m_z} \eta_{zi}(t) S_{zi}(x_4) \tag{2.6}$$

where

η_{yi}, η_{zi} – unknown functions of time

S_{yi}, S_{zi} – known functions of the coordinate x_4, connected with the form of jib oscillations.

As a result of the proposed method the number of generalized coordinates can be reduced from $e = e_y + e_z$ to $m = m_y + m_z$. Due to this the number of jib degrees of freedom diminishes radically although the basic dynamic properties are preserved (first m frequencies and forms of free vibrations). Based upon

Eqs (2.6), the position vector of a particular point of the flexible part of the jib can be written, in the inertial coordinate system, by means of the formula

$$\boldsymbol{r} = \mathbf{B}_s \mathbf{B}_u \overline{\boldsymbol{r}}_4 \tag{2.7}$$

where

- $\overline{\boldsymbol{r}}_4$ – vector of the jib point position before deformation, expressed in the coordinate system $0_4X_4Y_4Z_4$, $\overline{\boldsymbol{r}}_4 = [\overline{x}_4, \overline{y}_4, \overline{z}_4, 1]^\top$
- $\boldsymbol{r}$ – position vector expressed in the coordinate system $0XYZ$, $\boldsymbol{r} = [x, y, z, 1]^\top$
- $\mathbf{B}_u$ – matrix operator 4×4, which describes deflection of the jib
- $\mathbf{B}_s$ – matrix operator 4×4, in which the change of the coordinate system from $0_4X_4Y_4Z_4$ to the inertial coordinate system is taken into consideration.

The potential energy V_O of the upper structure is a sum of the potential energy of the gravity forces V_{OG} and elastic deformation of the jib V_{E4}

$$V_O = V_{OG} + V_{E4} \tag{2.8}$$

The potential energy of the gravity forces can be written using the following formula

$$V_{OG} = V_{OG2} + V_{OG3} + V_{OG4} \tag{2.9}$$

where

$$V_{OG2} = m_2 g \mathbf{D}_0^\top {}_2^0\mathbf{B} \boldsymbol{r}_{c2} \qquad V_{OG3} = m_3 g \mathbf{D}_0^\top {}_3^0\mathbf{B} \boldsymbol{r}_{c3}$$

$$V_{OG4} = g \mathbf{D}_0^\top \int_{m_4} \boldsymbol{r}\, dm_4 \qquad \mathbf{D}_0^\top = [0, 0, 1, 0]$$

and

- $\boldsymbol{r}_{c2}$ – coordinates of the centre of gravity of the elements connected with the upper structure expressed in the $0_2X_2Y_2Z_2$ coordinate system, $\boldsymbol{r}_{c2} = [x_2^c, y_2^c, z_2^c]^\top$
- $\boldsymbol{r}_{c3}$ – coordinates of the centre of gravity of the non-deformable elements of the jib expressed in the $0_3X_3Y_3Z_3$ coordinate system, $\boldsymbol{r}_{c3} = [x_3^c, y_3^c, z_3^c]^\top$
- $\boldsymbol{r}$ – position vector of the jib point, defined in Eq. (2.7).

It was assumed that the jib is modelled by a variable cross-section beam of the lenght L_w. The following expression describes the potential energy of jib deformation

$$V_{E4} = \frac{1}{2} \int_0^{L_w} \left[E_{mw} I_y \left(\frac{\partial^2 z_4}{\partial x_4^2} \right)^2 + E_{mw} I_z \left(\frac{\partial^2 y_4}{\partial x_4^2} \right)^2 \right] dx_4 \tag{2.10}$$

where

E_{mw} – Young's modulus of the jib material

$I_y = I_y(x_4)$ – inertial moment of the jib cross-section towards the axis Y_4

$I_z = I_z(x_4)$ – inertial moment of the jib cross-section towards the axis Z_4.

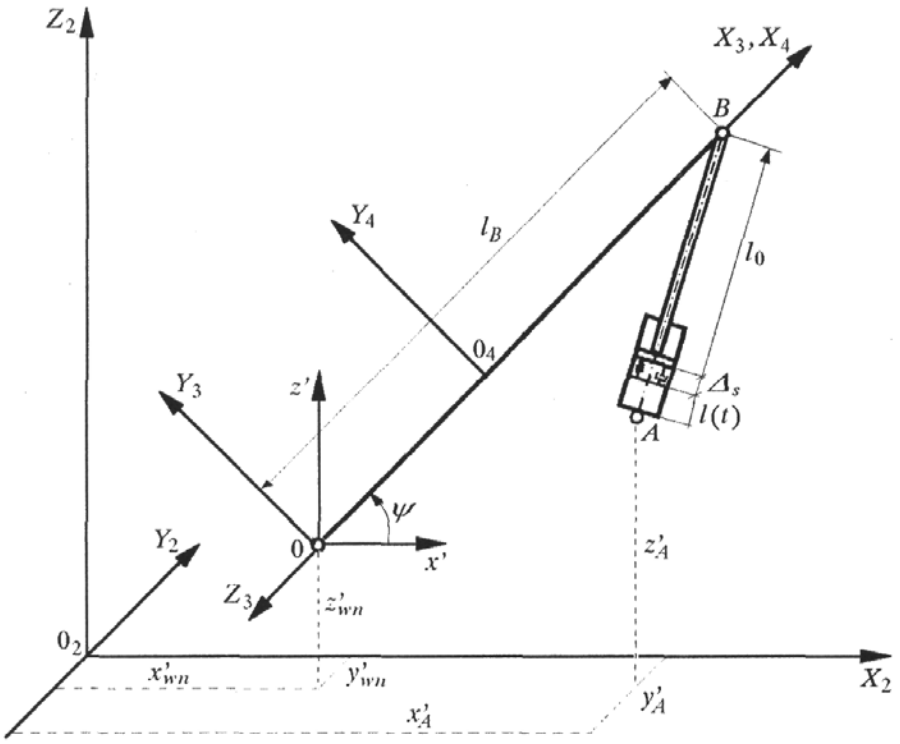

Fig. 4. Model of hydraulic servo-motor changing the crane radius

2.3. Model of the servo-motor changing the crane radius

In modelling the hydraulic servo-motor which changes the crane radius (Fig. 4), the following assumptions have been made:

- the points 0_3, A and B lie in a parallel plane to the $0_2X_2Z_2$ plane,
- the function $l(t)$ as well as its derivatives are given,
- flexibility and damping of the servo-motor can be reduced to a single spring-damping element,
- influence of kinetic energy throught about by relative motion of the servo-motor elements on motion of the system is neglected,

- mass changes of the liquid in the servo-motor cylinder are small in comparison to its whole mass,
- the deflection of the servo-motor Δ_s is equal to zero in the case of lack of the load.

The potential energy of the gravity forces can be treated as a sum

$$V_{sg} = V_{sg1} + V_{sg0} \tag{2.11}$$

where

$$V_{sg1} = m_{s1} g [0, 0, 1, 0] \boldsymbol{r}_{c1} \qquad V_{sg0} = m_{s0} g [0, 0, 1, 0] \boldsymbol{r}_{c0}$$

and

m_{s1}, m_{s0} – masses of undisplaced and displaced parts of the servo-motor, respectively

$\boldsymbol{r}_{c1}, \boldsymbol{r}_{c0}$ – position vectors of the centres of gravity of both parts.

The elastic deformation energy and the function of its dissipation can be written as

$$V_{ss} = \frac{1}{2} c_S \Delta_s^2 \qquad D_s = \frac{1}{2} b_S \dot{\Delta}_s^2 \tag{2.12}$$

where

c_S, b_S – stiffness and damping coefficients of the servo-motor.

2.4. Model of the rope system. Contact of the load with the ground

The load is modelled as a particle. In further considerations, certain elasticity of the rope within segments WG and GL is assumed (Fig. 6).

The potential energy of deformation of the rope and its function of dissipation can be calculated by the formulae

$$V_l = \frac{1}{2} \delta c_l \Delta_l^2 \qquad D_l = \frac{1}{2} \delta b_l \dot{\Delta}_l^2 \tag{2.13}$$

where

$$\delta = \begin{cases} 0 & \Rightarrow \quad \Delta \leqslant 0 \\ 1 & \Rightarrow \quad \Delta > 0 \end{cases}$$

and

Δ_l – deformation of the rope

c_l, b_l – rope stiffness and damping coefficients.

The phases of lifting a load from the ground and phases of putting it down are investigated in order to analyse the full working cycle of the crane. In

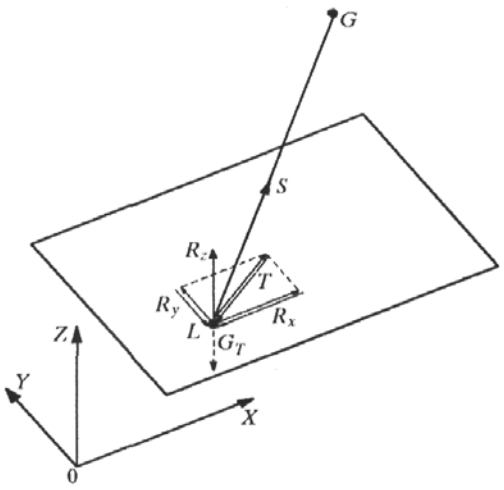

Fig. 5. Forces acting on the load at the moment of its contact with the ground

Fig. 5 $\boldsymbol{S} = [S_x, S_y, S_z, 1]^\top$ denotes the force in the rope, G_L – gravity force acting on the load, T – friction force, $\boldsymbol{R} = [R_x, R_y, R_z, 1]^\top$ reaction forces. In formulating the equations of motion for the load, the following three cases should be taken into consideration:

1. $R_z \leqslant 0$ – the load has no contact with the ground – it has three degrees of freedom
2. $R_z > 0$ and $\sqrt{S_x^2 + S_y^2} < \mu R_z$ – the load lies motionless on the ground
3. $R_z > 0$ and $\sqrt{S_x^2 + S_y^2} \geqslant \mu R_z$ – the load is moving over the ground – it has two degrees of freedom

where μ – coefficient of Coulomb's friction.

2.5. Models of drives

The input force in the slewing motion of the upper structure is assumed to be a kinematic force via a parallel system of elements: elastic and damping (Kelvin-Voigt's model). In Fig. 6 the following denotations were used:

c_{SR}, b_{TR} – stiffness and damping coefficients of the slewing mechanism for the upper structure

φ_w – kinematic force angle of the slewing of the upper structure (variable as a function of time).

The potential energy and the function of dissipation of the slewing motion drive are determined as

$$V_{SR} = \frac{c_{SR}(\varphi - \varphi_w)^2}{2} \qquad D_{TR} = \frac{b_{TR}(\dot{\varphi} - \dot{\varphi}_w)^2}{2} \tag{2.14}$$

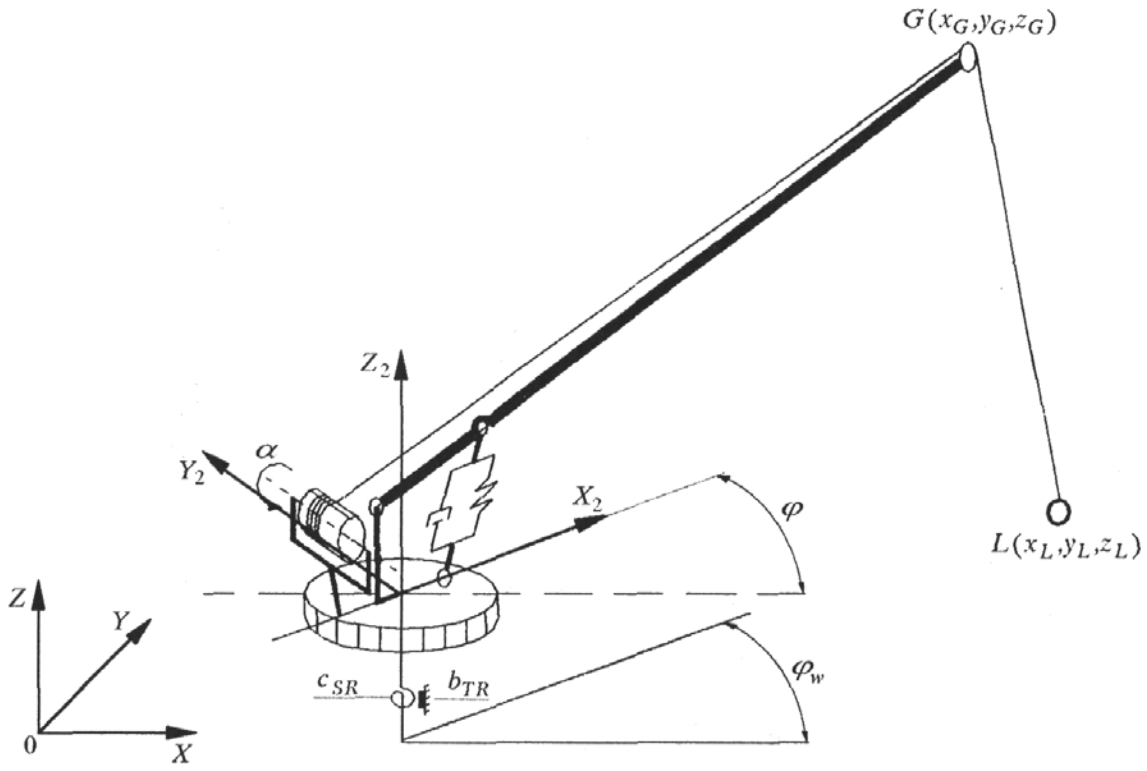

Fig. 6. Model of the rope system, load and input drive of slewing

The mechanism of the hoisting winch is modelled in a similar way, so

$$V_{SB} = \frac{c_{SB}(\alpha - \alpha_w)^2}{2} \qquad D_{TB} = \frac{b_{TB}(\dot{\alpha} - \dot{\alpha}_w)^2}{2} \tag{2.15}$$

where

V_{SB}, D_{TB} – potential energy and the function of dissipation of the hoisting winch drive

c_{SB}, b_{TB} – stiffness and damping coefficients of the hoisting mechanism

α_w – kinematic force of the hoisting drum (variable as a function of time).

2.6. Equations of motion

After determination of all necessary components of the Lagrange equations, the following system of equations of motion is obtained

$$\mathbf{A}_w \ddot{\boldsymbol{w}} = \boldsymbol{F} \tag{2.16}$$

which can be rewritten in the following form

$$\underbrace{\begin{bmatrix} A^p & A^{wqp} & 0 & 0 \\ A^{wpq} & A^{wpp} & 0 & 0 \\ 0 & 0 & A^b & 0 \\ 0 & 0 & 0 & A^L \end{bmatrix}}_{\mathbf{A}_w} \underbrace{\begin{bmatrix} \ddot{q} \\ \ddot{p} \\ \ddot{\alpha} \\ \ddot{q}^L \end{bmatrix}}_{\ddot{\boldsymbol{w}}} = \underbrace{\begin{bmatrix} F^q \\ F^p \\ F^B \\ F^L \end{bmatrix}}_{\boldsymbol{F}} \tag{2.17}$$

where

- $\boldsymbol{q}$ – vector of coordinates called stiff coordinates, $\boldsymbol{q} = [q_1, ..., q_6, \varphi, \psi]^\top$
- $\boldsymbol{p}$ – vector of coordinates of the jib, $\boldsymbol{p} = [p_1, ..., p_{m_y}, p_{m_y+1}, ..., p_{m_y+m_z}]^\top$
- m_y, m_z – number of modes taken into consideration in modal analysis, in the plane of lifting and in the plane perpendicular to it, respectively
- $\boldsymbol{q}^L$ – vector of coordinates of the load that may have zero, two or three elements.

The necessary non-zero elements of the matrices $\mathbf{A}_w$ and vector $\boldsymbol{F}$ are calculated on the grounds of equations presented in Sections 2.1-2.5. More information about the mathematical model is given in Maczyński (2000). Equations (2.16) form a system of ordinary non-linear differential second-order equations for variable t. Before they can be solved, the static deflections should be determined since these constitute initial conditions for motion of the system.

The fourth order Runge-Kutta method was used to solve the system of differential equations (2.16). An appropriate computer program was prepared using DELPHI v. 4.0 algorithmic language together with a user interface for convenient data input and visualisation of results. It can be used for dynamic analysis of a wide range of mobile cranes (particularly with a telescopic jib) and also other types of cranes such as floating off-shore cranes and on-shore cranes.

3. Description of the ADAMS model

The second model (Fig. 7) is developed using the commercial ADAMS/View® package. Similar assumptions have been made but the investigations are restricted to rotation of the upper structure. The chassis is

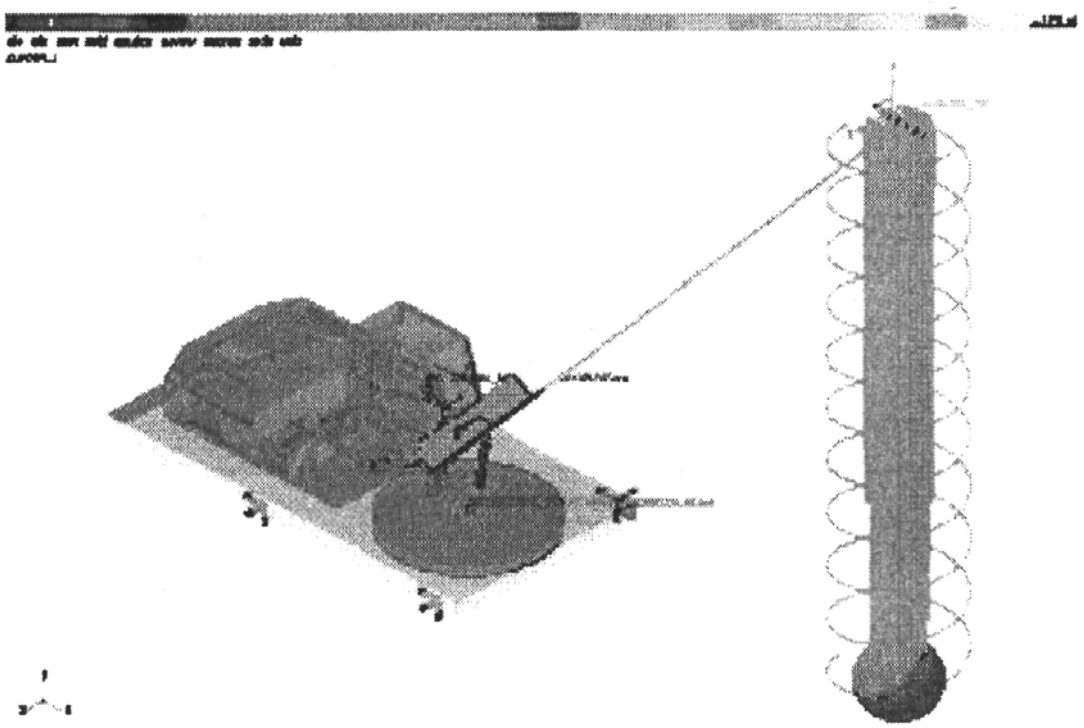

Fig. 7. Model of the crane using ADAMS®

a rigid body supported on flexible supports modelled as a system of parallel spring-dampers acting in the directions X, Y and Z of the global system of coordinates. These are standard *spring* elements with linear characteristics of stiffness and damping. In order to model the telescopic jib (*flexible body*), the ANSYS® program is used which provides calculations by means of the finite element method. The model of the jib is build up out of the SOLID45 type elements with the length equal to 1/20 of the total length of the jib. After the modal analysis in the ANSYS® system, the results are transferred via the ADAMS/Flex® program to the ADAMS/View® package. Only the first two forms of vibrations are stored. During translation the results undergo very slight changes; this has a small effect on the final results of calculations. The rotary upper structure and chassis are connected by a *revolute joint* with its stiffness modelled by a *torsional spring*. The servo-motor that changes the crane radius is replaced by rigid elements representing the immobile part (cylinder) and the mobile part (piston rod). These elements are connected (*translational joint*) by one spring-damping element modelling stiffness and damping of the servo-motor. The rope (its section from the tip of the jib to the load) is also modelled as a linear *spring* element. The drive function of the rotary upper structure of the crane is defined discretely by means of a spline (*Akima's method*) and represented by the object *rotational motion*.

4. Numerical simulations and analysis of the results

Numerical calculations for both models have been carried out assuming the geometry and mass parameters defined in the specifications of the DUT 0203 crane and accessible literature. The DUT 0203 crane is one of the most popular Polish cranes with a capacity up to 30 Mg. Detailed information about choice of the model parameters can be found in Maczyński (2000). The simulations assumed: load mass 4500 kg, jib length 16 m, initial height of the load above the ground 2 m, angle of jib inclination 50°. Rotation of the upper structure through 90° over 15 s was analysed. The drive function in Fig. 8 was previously optimised in terms of minimalization of final load oscillations (Maczyński and Wojciech, 2000).

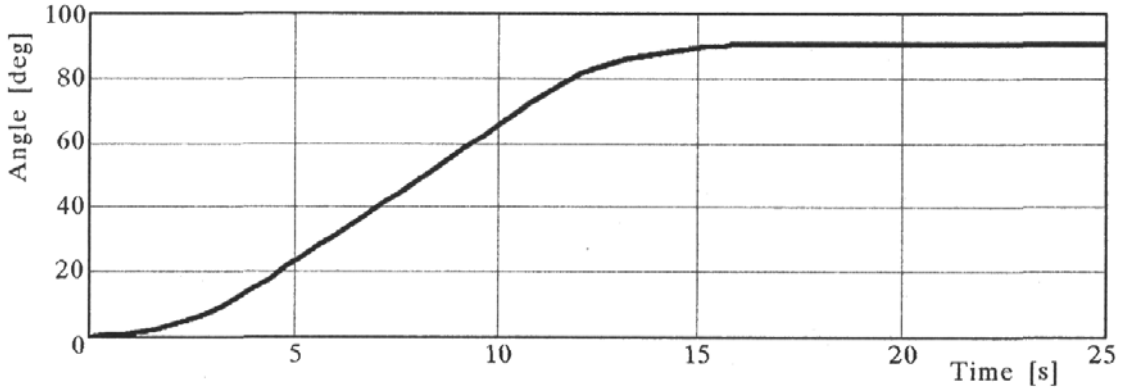

Fig. 8. Drive function of rotation of the upper structure after optimisation ($t = 15$ s)

On the graphs included in this Section the results obtained for the first model are denoted as CRANE and for the second as ADAMS.

A quantity, which accurately reflects the dynamic loads in the system, is the dynamic coefficient of the force in the rope. It is defined as follows

$$\eta = \frac{S}{mg} \tag{4.1}$$

where

S – dynamic force in the rope

m – mass of the load.

therefore, this coefficient defines the dynamic to static load ratio. The time history of the coefficient η during rotation of the upper structure and for 105 s after the end of motion is given in Fig. 9. If we compare these histories we can see that at the initial stage of motion the dynamic loads obtained with the ADAMS model are higher but in course of time these values quickly become

similar to those obtained with the CRANE model. It is important to stress that in both cases the obtained histories have the same period.

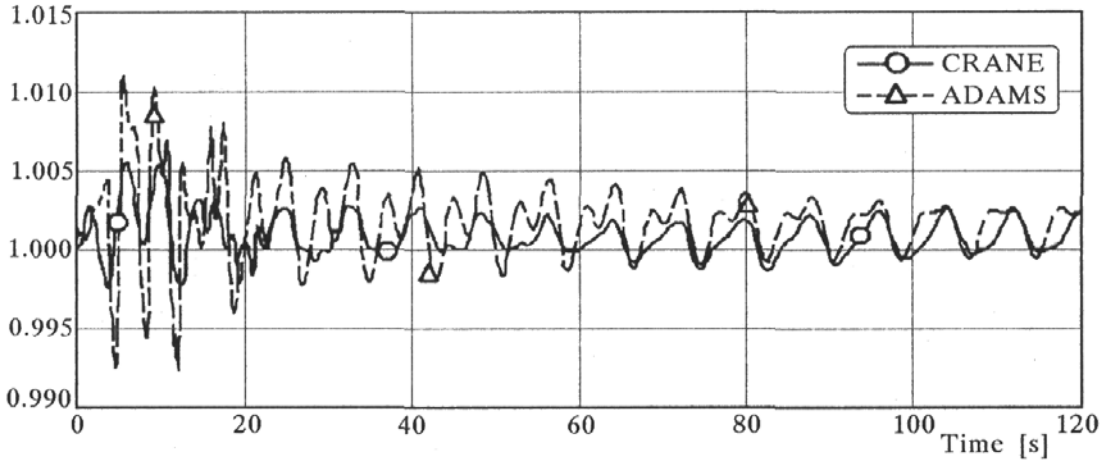

Fig. 9. Time history of the dynamic coefficient of the force in the rope

The first model (Fig. 1) was used in Maczyński (2000) to investigate the effectiveness of an algorithm to minimalise the final load oscillations during rotation of the upper structure. The load trajectory is essential for this, and especially its projection on the horizontal plane. A comparison in this respect for the two models is shown in Fig. 10.

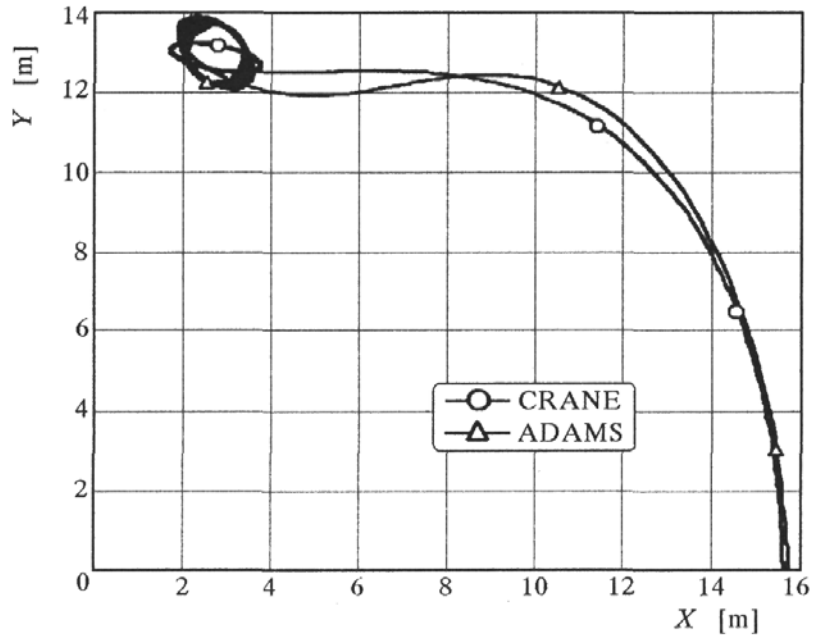

Fig. 10. Projection of the trajectory of the load on the horizontal plane

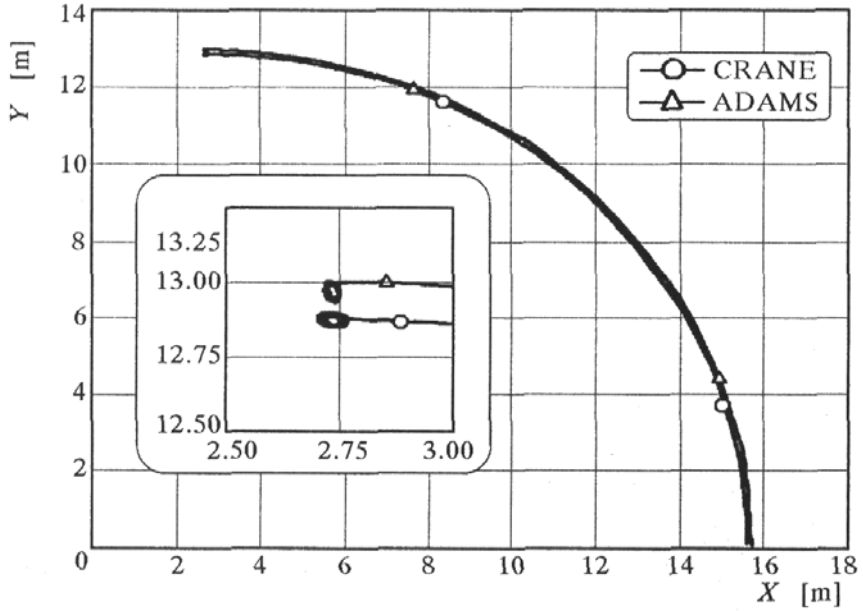

Fig. 11. Projection of the trajectory of the point G (tip) of the jib on the horizontal plane

Fig. 11 presents the projection of the trajectory of the jib tip (point G in Fig. 1) on the horizontal plane. The load magnifies the final stage of the trajectories investigated.

It can be seen from Figs. 10 and Fig. 11 that similar trajectories of the load and point G of the jib are obtained. In the ADAMS model the final oscillations of the load are slightly greater than in the CRANE model. The final oscillations of the point G of the jib are, however, virtually the same; in the ADAMS model there is simply a small outward displacement of both trajectories in relation to the trajectories obtained for the CRANE model (about 12 cm). The discrepancy between the good correspondence for the point G and the worse correspondence for load largely results from the different method for modelling the rope. In the ADAMS® system it is modelled as a parallel connection of a spring and a damping element. In the CRANE model it is massless and limp, and the energy of its flexible deformation and function of dissipation is calculated at every step for the actual length of the working rope.

Figure 12 shows the time history of the dynamic coefficient of the force in the servo-motor that changes the crane radius. This coefficient is defined by the dynamic to static force ratio

$$\eta_s = \frac{S_s^d}{S_s^s} \tag{4.2}$$

where
S_s^d – dynamic force in the servo-motor
S_s^s – static force in the servo-motor caused by its own weight and the load.

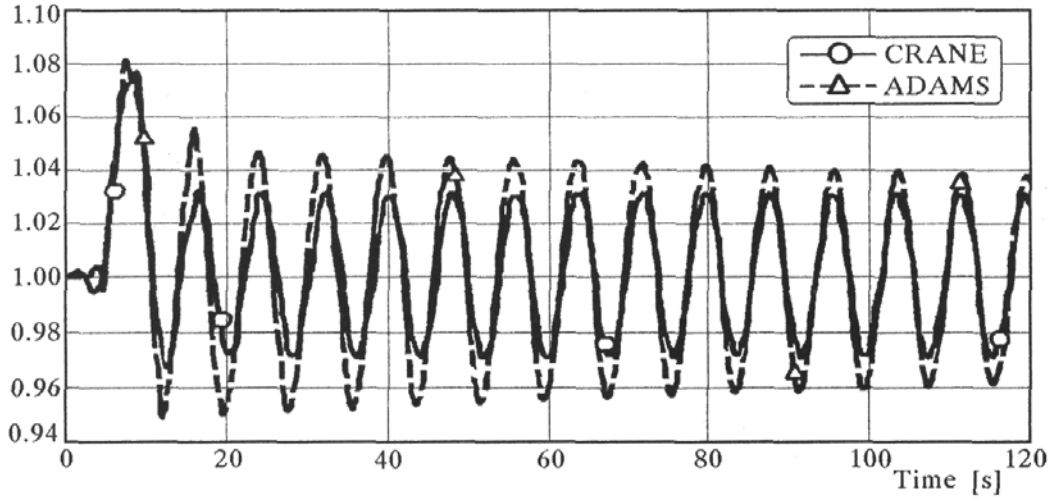

Fig. 12. Comparison the dynamic coefficient of the force in the servo-motor changing the crane radius

In both cases the curves have been obtained with the same frequency, and with amplitudes which differed by 50% at the most. In the course of time, however, the amplitude values quickly become similar.

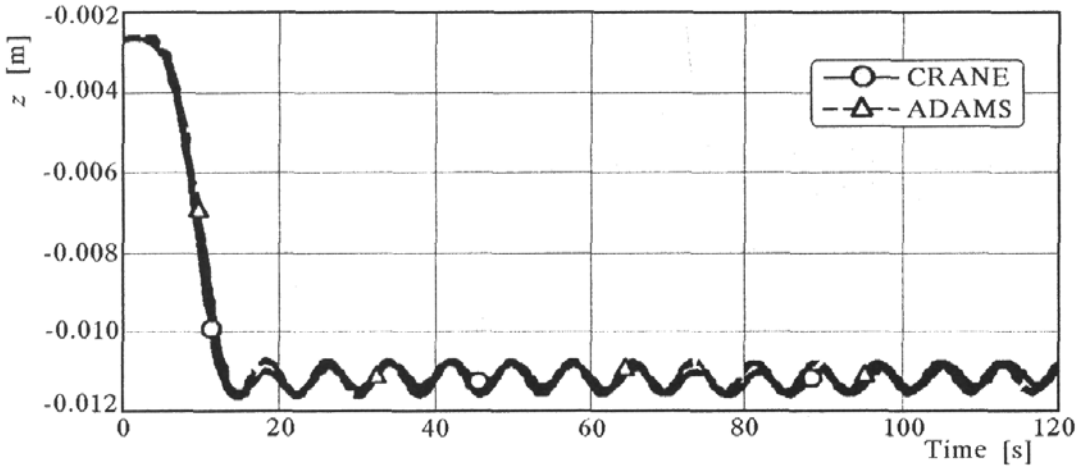

Fig. 13. Time history of the coordinate z of the chassis

The following graphs enable the movements of the chassis to be compared by showing the time histories of the coordinates z and y of the centre of gravity

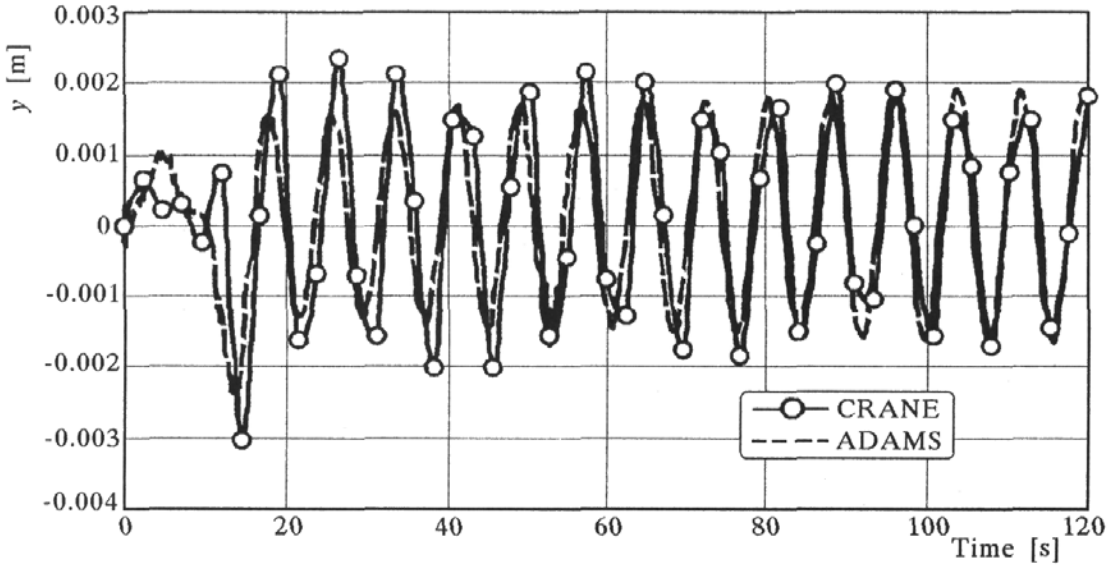

Fig. 14. Time history of the coordinate y of the chassis

of the chassis (Fig.13 and Fig. 14), and the angle of rotation in relation to $0X$ axis (Fig. 15). The results demonstrate that there are only slight differences between the models in describing the displacement of the chassis.

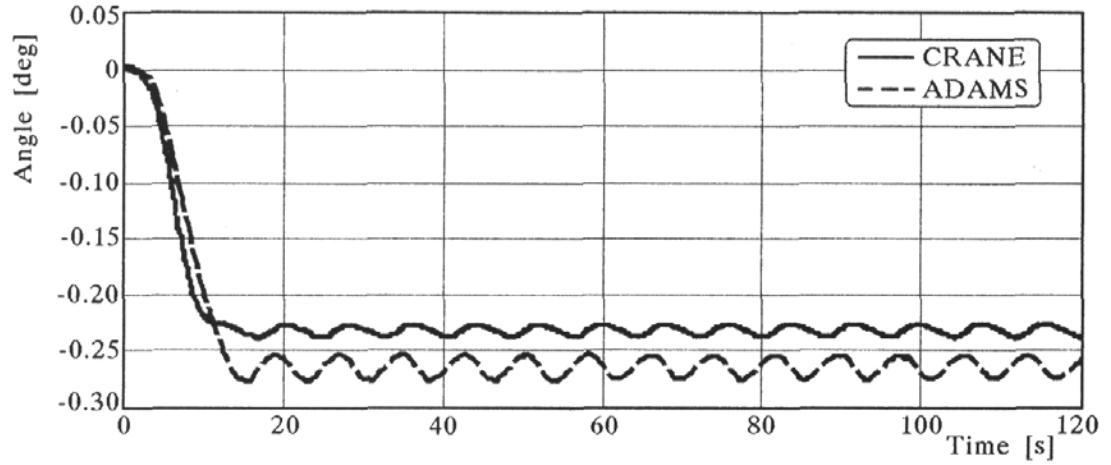

Fig. 15. Time history of the angle of rotation of the chassis about the $0X$ axis

5. Concluding remarks

The graphs in the previous section demonstrate a large degree of convergence of the results of both models. The last three examples (Fig. 13 ÷ Fig. 15)

confirm the particularly good correspondence of both models for the bearing structure of the crane (chassis, support system, rotary upper structure, jib and servo-motor changing the crane radius). Slightly greater discrepancy is found in the dynamic analysis of the load and rope; this is mainly caused by differences between the two methods of modelling the rope. Nevertheless, the curves obtained (e.g. Fig. 12 – dynamic coefficient) have very similar frequencies.

The ADAMS® package is superior in terms of simulation time. It is essential to choose the correct integration step for the equations of motion. The CRANE program requires an integration step of the order of 10^{-3} s, but ADAMS® has automatic step selection, which enables the comparative model to be analysed in a shorter time (about 30% difference).

Constructing a complex crane model with ADAMS® requires good knowledge of the system. The time necessary to construct the model is without doubt longer than filling in edit fields in the CRANE program equipped with a convenient user interface. In the CRANE model the dynamics of the flexible jib is investigated by modal analysis; in the ADAMS model the jib is defined in the ANSYS® program, which entails even more time and work spent in familiarising oneself with this system. An additional problem is the transfer of data from ANSYS® to the ADAMS® system; this can lead to erroneous results. The use of numerically effective modal analysis in the CRANE program means that the researcher can investigate jib vibrations and their effect on the whole system without investing additional time and effort, which is an important advantage of this program. In both methods it is easy to change the features and parameters of the model. However, it is more difficult to change or reconstruct the actual structure of the model in the CRANE program since this would require changing of the source code. The ADAMS® is superior in this respect and it is relatively easy to change the structure or add new components to the model. For instance, it is quite non-problematic in the ADAMS® to add an uneven base surface but in the case of the CRANE program it would require quite large changes in the modelling and programming. In the light of these considerations it can be stated that the CRANE program is suitable for carrying out calculations for many variants at the design stage since it is simple and quick to construct the model. The time saved in the process of constructing the model is enormous in relation to the ADAMS®, which requires huge time and effort from the user's part.

The numerical verification reveals a large degree of correspondence between the models for the rotation of the upper structure and demonstrates that both models correctly describe the dynamics of a crane with that type of the input function. This is particularly important for the authors because the CRANE

model was used in Maczyński (2000) to develop control strategies for the rotation of the upper structure which ensured minimization of the final load oscillations. In the future research the authors intend to expand the model developed in the ADAMS® system so that it can be used to verify other working movements of the crane.

References

1. CHWASTEK S., MICHAŁOWSKI S., 2000, Przestrzenny model żurawia na podłożu kołowym dla analizy obciążeń trakcyjnych z uwzględnieniem podatności ramy, *Proceedings of XIII Konferencji Problemy Rozwoju Maszyn Roboczych*, Zakopane, Tom I, 97-104

2. CHWASTEK S., MICHAŁOWSKI S., 2001, Suppression of crane vibrations with controlled boom support system, *The Archive of Mechanical Engineering*, **XLVIII**, 1, 19-27

3. GRABSKI J., STRZAŁKO J., TROMBSKI M., 1993, Badanie wrażliwości strukturalno-modelowej żurawia, *Proceedings of IV Ogólnopolskiej Konferencji Mechaniki Maszyn Włókienniczych i Dźwigowych, Bielsko-Biała, Zeszyty Naukowe Politechniki Łódzkiej Filii w Bielsku-Białej*, 96-101

4. GRABSKI J., STRZAŁKO J., TROMBSKI M., 1994, Przestrzenny model żurawia, równania Boltzmanna Hamela, *Proceedings of VII Konferencji Problemów Rozwoju Maszyn Roboczych*, Zakopane, 17-20 stycznia 1994, Tom I, 187-192

5. HARLECKI A., 1998, Dynamic analysis of telescopic truck crane using the rigid finite element method, *Zeszyty Naukowe Politechniki Łódzkiej Filii w Bielsku-Białej, Budowa i Eksploatacja Maszyn*, **51**, 32, 11-39

6. HO-HOON L., 1998, Modelling and control of a three-dimensional overhead crane, *Journal of Dynamic Systems, Measurement, and Control*, **120**, 471-476

7. KŁOSIŃSKI J., 2002, Wpływ typu i nastaw regulatora na właściwości dynamiczne układu regulacji ruchu obrotowego żurawia, *Przegląd Mechaniczny*, **1**, 21-24

8. KOŚCIELNY R., WOJCIECH S., 1994, Nonlinear vibration of the subsystem in various media conditions, *Structural Dynamics and Vibration*, PD-**63**, 47-52

9. KUKLA S., POSIADAŁA B., PRZYBYLSKI J., 1994, Analiza drgań swobodnych wysięgnika teleskopowego, *Proceedings of VI Konferencji Naukowej Sterowanie, napęd, wytrzymałość zmęczeniowa i projektowanie maszyn budowlanych, Część II, Napęd, modelowanie i badania*, Rynia, 91-98

10. LUBNAUER W.A., GRABSKI J., STRZAŁKO J., 1996, Wpływ charakterystyk układu napędowego na proces sterowania ruchem ładunku, *Proceedings of IX Konferencji Problemy Rozwoju Maszyn Roboczych i VIII Konferencji Naukowej Problemy w Konstrukcji i Eksploatacji Maszyn Hutniczych i Ceramicznych*, Zakopane, zeszyt IV, 73-80

11. MACZYŃSKI A., 1998, Porównanie różnych modeli wysięgnika teleskopowego zbudowanych z wykorzystaniem MES, *Zeszyty Naukowe Politechniki Łódzkiej Filii w Bielsku-Białej, Budowa i Eksploatacja Maszyn*, **32**, 51, 61-70

12. MACZYŃSKI A., 2000, Dynamika żurawia samojezdnego w aspekcie sterowania jego napędami, Ph.D. Thesis, Technical University of Łódź in Bielsko-Biała

13. MACZYŃSKI A., KOŚCIELNY R., 1999, A dynamic model to pptimisation working motions of a mobil crane, *Proceedings Tenth World Congress on the Theory of Machines and Mechanisms*, Finland, Oulu, **4**, 1561-1566

14. MACZYŃSKI A., SUWAJ S., 1993, Porównanie metod wyznaczania parametrów zastępczych wysięgnika teleskopowego, *Proceedings of IV Ogólnopolskiej Konferencji Mechaniki Maszyn Włókienniczych i Dźwigowych, Bielsko-Biała, 1993, Zeszyty Naukowe Politechniki Łódzkiej Filii w Bielsku-Białej*, 189-194

15. MACZYŃSKI A., WOJCIECH S., 2000, Dobór funkcji określającej obrót żurawia w celu minimalizacji wahań ładunku, *Proceedings. of the XII Conference on "Drives, Control and Automation of Working Machines and Vehicles"*, Rynia by Warsaw, 317-326

16. MAJEWSKI L., TROMBSKI M., 1993, Przestrzenny model dźwigu z uwzględnieniem luzu w parach kinematycznych wysięgnika teleskopowego, *Proceedings of IV Ogólnopolskiej Konferencji Mechaniki Maszyn Włókienniczych i Dźwigowych, Bielsko-Biała, Zeszyty Naukowe Politechniki Łódzkiej Filii w Bielsku-Białej*, 195-202

17. OSIŃSKI M., WOJCIECH S., 1994, Dynamic of hoisting appliances in maritime conditions, *Machine Vibration*, **3**, 76-84

18. OSIŃSKI M., WOJCIECH S., 1996, Some problems of dynamic analysis and control of an off-shore crane, *Proceedings of the 5th International Conference of Cranes and Textile Machines EUROCRANE'96*, Gdańsk, 114-125

19. OSIŃSKI M., WOJCIECH S., 1998, Application of nonlinear opitmisation methods to input shaping of the hoist drive of an off-shore crane, *Nonlinear Dynamics*, **17**, 369-386

20. PARKER G.G., GROOM K., HURTADO J. E., FEDDEMA J., ROBINETT R.D., LEBAN F., 1999a, Command shaping boom crane control system with nonlinear inputs, *Proceedings of the IEEE International Conference on Control Applications*, Hawai, 1774-1778

21. PARKER G.G., GROOM K., HURTADO J.E., FEDDEMA J., ROBINETT R.D., LEBAN F., 1999b, Experimental verification of a command shaping boom crane control system, *Proceedings of the American Control Conference*, San Diego, California, 86-90

22. PARKER G.G., PETTERSON B., DOHRMANN R.D., 1995a, Vibration suppression of flexed-time jib crane maneuvers, *Proceeding of the SPIE Symposium on Smart Structures and Materials*, **24471**, San Diego, 131-140

23. PARKER G.G., ROBINETT R.D., DRIESSEN B.J., DOHRMANN R.D., 1995b, Operator in-the-loop control of rotary cranes, *Proceeding of the SPIE Symposium on Smart Structures and Materials*, **2721**, San Diego, 364-372

24. POSIADAŁA B., SKALMIERSKI B., TOMSKI L., 1991, Dynamical models of the truck crane telescopic booms, *Abstracts of 1st European Solid Mechanics Conference*, p. 162

25. POSIADAŁA B. ET AL., 2000, *Modelowanie i badanie zjawisk dynamicznych wysięgników teleskopowych i żurawi samojezdnych*, WNT, Fundacja Książka Naukowo-Techniczna, Warszawa, 1-155

26. SAKAWA Y., NAKAZUMI A., 1985, Modelling and control of a rotary crane, Journal of Dynamic Systems, *Measurement and Control*, **107**, 200-206

27. SAKAWA Y., SHINDO Y., HASHIMOTO Y., 1981, Optimal control of a rotary crane, *Journal of Optimzation Theory and Applications*, **35**, 4, 535-557

28. TANIZUMI K., YOSHIMURA T., HINO J., SAKAI T., 1995, Modelling of dynamic behaviour and control of truck cranes (sway and velocity control of truck cranes with hydraulic system in swing operation), *Transactions of the Japan Society of Mech. Eng.*, **61**, 540-556, 4629-4637

29. TOWAREK Z., 1996a, Dynamic of a crane on a soil foundation as a function of carrier force, *Machine Vibration*, **5**, 211-223

30. TOWAREK Z., 1996b, Effect of non-linear soil on the dynamics of the crane during rope tightening, *Machine Dynamics Problems*, Warsaw University of Technology, **15**, 97-107

31. TOWAREK Z., TROMBSKI M., 1993, Dynamika żurawia wysięgnikowego podczas napinania liny z uwzględnieniem reologii podłoża, *Proceedings of IV Ogólnopolskiej Konferencji Mechaniki Maszyn Włókienniczych i Dźwigowych, Bielsko-Biała, 1993, Zeszyty Naukowe Politechniki Łódzkiej Filii w Bielsku-Białej*, 318-324

32. TOWAREK Z., TROMBSKI M., 1994, Wpływ podatności gruntu na dynamikę żurawia podczas napinania liny, *Proceedings of VII Konferencji Problemów Rozwoju Maszyn Roboczych*, Zakopane, Tom II, 255-260

33. TROMBSKI M. ET AL., 1990, *Optymalizacja układu podporowego żurawia samochodowego jako członu układu automatycznego sterowania ruchami roboczymi, Etapy: I, II, II, IV, Realizacja – Wyniki – Wnioski*, wykonana w ramach Prac Naukowego Centralnego Programu Badań Podstawowych 2.06, Temat nr 03.23.01, Wydawnictwo Politechniki Warszawskiej, Warszawa 1990

34. TROMBSKI M., TOWAREK Z., 1997, Dynamika żurawia posadowionego na gruncie w czasie obrotu wysięgnika, *Proceedings of X Konferencji Naukowej "Problemy rozwoju maszyn roboczych"*, Zakopane, zeszyt 1, 295-302

35. TROMBSKI M., KŁOSIŃSKI J., MAJEWSKI L., SUWAJ S., 1995, Some problems of controlling crane truck working movements, *Proceedings of Ninth World Congress on the Theory of Machines and Mechanisms*, Politecnico di Milano, Italy, **2**, 1411-1415

36. TROMBSKI M., KŁOSIŃSKI J., MAJEWSKI L., SUWAJ S., 1999, Sensitivity of the system controlling the working motions of a mobile crane to the disturbance signals, *Proceedings Tenth World Congress on the Theory of Machines and Mechanisms*, Finland, Oulu, **4**, 1578-1583

37. WOJCIECH S., 1993, Dynamic analysis of telescopic rapiers, *Machine Vibration*, **2**, 80-87

Porównanie modeli do analizy dynamicznej samojezdnego żurawia teleskopowego

Streszczenie

W pracy przedstawiono porównanie dwóch modeli samojezdnego żurawia teleskopowego. Pierwszy został opracowany na drodze analitycznej przy zastosowaniu metod z zakresu dynamiki manipulatorów z wykorzystaniem metody modalnej, drugi przy użyciu komercyjnego pakietu ADAMS®. Przedstawiono i porównano przykładowe wyniki symulacji numerycznych dla ruchu obrotowego nadwozia żurawia. Dokonano oceny modeli pod względem czasochłonności obliczeń, możliwości ich rozbudowy i zastosowania w projektowaniu żurawi.

Manuscript received January 17, 2002; accepted for print May 13, 2002